THE LUNAR NEUTRON LEAKAGE FLUX AND ITS MEASUREMENT BY LUNAR PROSPECTOR NEUTRON SPECTROMETERS. R. C. Elphic[1], W. C. Feldman[1], D. J. Lawrence[1], O. M. Gasnault[1], S. Maurice[2], R. Little[1], T. H. Prettyman[1], and A. B. Binder[3], [1]Los Alamos National Laboratory, Group NIS-1, MS D466, Los Alamos, NM 87544 (relphic@lanl.gov); [2]Observatoire Midi-Pyrénées, Toulouse, France; [3]Lunar Research Institute, Tucson, Arizona.

Introduction: Galactic cosmic rays interacting with surface materials of the Moon give rise to a population of nuclear products within the soils. Among these products are energetic neutrons that interact with surrounding nuclei, which moderate (downscatter in energy) and absorb the neutrons. Some of these neutrons leak out of the soil, and the parameters of this leakage flux depend upon the composition and temperature of the soil as well as cosmic ray flux [1,2]. It is important to understand how these composition- and temperature-dependent leakage fluxes are manifested as count rates in orbital neutron spectrometer measurements from Lunar Prospector. In this paper we take leakage flux energy spectra for six different soil compositions as calculated by Monte Carlo simulations [1], and propagate the neutron distribution up to orbital altitudes. We then convolve the orbital neutron distribution with the area-efficiency response function of the cadmium- and tin-covered ^{3}He proportional counter tubes used to measure the epithermal and thermal + epithermal neutrons, respectively [3].

Monte Carlo Simulations of Neutron Leakage Flux: The energy fluxes (neutrons $cm^{-2}\,s^{-1}\,eV^{-1}$) per fast neutron have been calculated in [1]. Six soil compositions have been simulated in that work: Apollo 11 basalt soil, Apollo 12 basalt soil, Apollo 17 soil, Apollo 17 high-Ti mare basalt soil, ferroan anorthosite (FAn), and Luna 20 soil. Each soil was simulated at four temperatures: 100, 200, 300, and 400 K. Figure 1 shows the leakage energy flux for the six soil compositions at 300 K. The energy flux

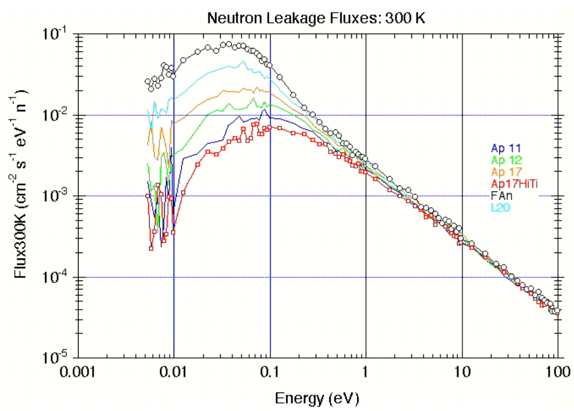

Fig. 1. Neutron leakage flux as a function of energy for six compositions

varies most at energies below about 0.3 eV, reflecting primarily the thermal neutron absorption due to iron and titanium. The Cd-covered (epithermal) detector should see relatively less variation in count rates, being sensitive to neutrons with energies above 0.3 eV. The Sn-covered (thermal + epithermal) detector is sensitive to the lower energies as well and should see considerably larger variations in count rate with soil composition.

Not shown here are the energy flux variations with soil temperature. In general, the peak amplitude and characteristic energy of the thermal part of the flux distribution decreases with soil temperature. This effect is most pronounced in low-iron compositions such as FAn and Luna 20.

Neutron Flux Distribution at Orbital Altitudes: Neutrons that leak out of the lunar soil follow ballistic trajectories above the surface, as in a classic planetary exosphere. Those with energies greater than the gravitational binding energy (0.029 eV) are lost to space, while those with energies below this value are gravitationally bound and follow closed orbits that re-encounter the surface at some point. In addition, neutrons decay with a 910 s characteristic decay lifetime, so quite a few gravitationally-bound neutrons decay before falling back to the surface.

We use the equations governing orbital mechanics to determine the trajectories and times of flight of the neutrons after leaving the surface, following the work of [4]. Conservation of angular momentum and energy govern the arrival energy and angle of the neutrons at orbital altitudes, while time of flight determines how many neutrons have decayed during flight from the surface.

Figure 2 shows the velocity-space representation of the neutron flux distribution for FAn at 300K, as seen at 100 km altitude. This figure displays a cut through a three-dimensional velocity distribution as seen in the frame of the spacecraft, with the velocity axes along the spacecraft trajectory (V_X) and vertical (V_Z). Note the offset from zero in V_X, which is due to spacecraft motion at 1.68 km/s. The speed corresponding to 0.3 eV is 7.6 km/s. Note that the greatest flux of neutrons is upward — the asymptotic lower limit of this upgoing flux corresponds to those trajectories that just intersect the lunar surface. Trajectories that do not intersect the lunar surface are, of

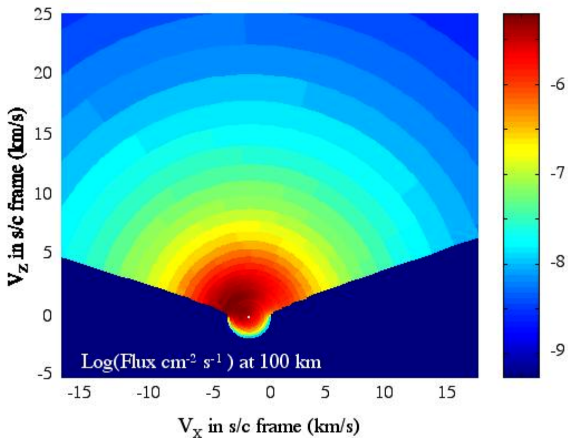

Fig 2. Log of neutron leakage flux at 100 km altitude, for FAn at 300 K.

course, devoid of neutrons. As the orbit altitude increases, this void zone grows in size, and the region of upward flux narrows. The downward flux is confined to neutrons with energies below the gravitational binding energy and that have not yet decayed. The hard lower limit on downgoing flux occurs at the escape velocity of about 2.36 km/s (neutrons with higher speeds escape, and never come down).

Comparison With LP Neutron Count Rates : The area-efficiency response of the LP neutron spectrometers as a function of energy and incidence angle to the Sn- and Cd-covered ^{3}He tubes has been estimated using both laboratory data and Monte Carlo calculations.. At energies below 0.1 eV, the Sn-covered tube has an area-efficiency of about 100 counts cm^2 per incident neutron at 90¡ incidence (normal to the tube axis), and falls off roughly as $E^{-1/2}$ at higher energies. The Cd-covered tube has a very rapid rise from zero to about 65 counts cm^2 per incident neutron at 90¡ incidence at 1 eV. Above this energy both tubes respond identically. For both tubes, this area-efficiency factor at low energies decreases as the incidence angle decreases until, at end-on orientations, the factor is a fraction of the normal-incidence case. At higher energies the tubes begin to act more as volume collectors, and the response becomes more uniform with incidence angle.

The three-dimensional flux distribution at orbital altitudes can be convolved with the instrument area-efficiency response functions to create estimated neutron count rates in the two spectrometers. Some results can be found in Table 1, which shows the Cd- and Sn-covered tube count rates (HeCd and HeSn, in counts/s) for selected compositions and temperatures at 30 km altitude. The bottom two entries correspond to the observed LP neutron spectrometer minimum and maximum observed values at 30 km altitude. Also shown is the epithermal-to-thermal count rate ratio. Notice that for the more mafic compositions, temperature has a relatively minor effect on count rate, a matter of 2 or 3%. But for the FAn case, the difference between a 100 and 300K soil temperature amounts to a nearly 8% change in HeSn count rate. This means it may be possible to sense the difference between equatorial and polar subsurface soil temperatures. However, other complications need to be considered as well, such as the presence of polar hydrogen and the possibility of composition differences between equatorial and polar soils.

A final point is that these simulated count rates agree reasonably well with the range of count rates observed by the LP neutron spectrometers. This implies that the instrument response models, neutron leakage flux calculations, cosmic ray fast neutron yield estimates, and the description of neutron ballistics above the surface used here are all reasonably accurate.

References: [1]˚Little et al. (2001) this conference; [2] Feldman et al., (2000) *JGR*, 105 #E8, 20347—20363; [3]˚Feldman et al., (1999) *NuclInstrum. Methods Phys. Res., Sect. A*, 422, 562-566; [4] Feldman, et al., (1994) *JGR*, 94, 513-525.

Table 1. Calculated and Observed Count Rates

Comp.	T (K)	HeCd	HeSn	Epi/th
Ap11	100	13.9	20.5	2.09
Ap11	300	14.3	21.2	2.07
HiTi	100	13.6	18.8	2.58
HiTi	300	13.7	19.2	2.53
FAn	100	16.7	39.2	0.74
FAn	300	17.3	42.1	0.70
LP min	-	16.5	25.5	0.83
LP max	-	19.2	44.9	2.55